

ARTICLE OPEN



Chemogenetic modulation of the prelimbic cortex to the nucleus accumbens core pathway reduces cocaine-induced increase of risk preference

Joonyeup Han^{1,2}, Myung Ji Kwak^{1,2,3}, Wha Young Kim¹✉ and Jeong-Hoon Kim^{1,2}✉

© The Author(s) 2026

Decision-making impairments are a core symptom of several psychiatric disorders, including gambling and substance use disorders (SUD). These disorders frequently co-occur, suggesting shared neurobiological mechanisms underlying dysfunctional decision-making. We previously demonstrated that chronic cocaine exposure increases risk preference in a rat gambling task (rGT). Given that the prelimbic cortex (PrL) to the nucleus accumbens (NAc) core pathway plays a crucial role in regulating risk-based decision-making, we further explored how chemogenetic modulation of this pathway alters cocaine-induced increase in risky decision-making in the rGT. Notably, activation of Gi, but not Gq, designer receptors exclusively activated by designer drugs (DREADD) in the PrL attenuated the cocaine-induced increase of risk preference in risk-averse rats, while simultaneously reducing cocaine-induced attentional deficits measured by task omissions. Subsequent molecular analyses revealed that cocaine significantly induced changes in the expression levels of calcium channel alpha 1 C subunit (CaV1.2) and in the ratio of phosphorylation at serine 97 of total dopamine- and cAMP-regulated phosphoprotein, 32 kDa (DARPP-32) in the PrL region of these rats, which returned to basal levels with concurrent Gi-DREADD activation. No significant behavioral or molecular changes were observed in risk-seeking rats. These results suggest that modulating the PrL-NAc core pathway can selectively control risk-based decision-making behavior and attentional processes affected by cocaine exposure, offering therapeutic potential for addressing decision-making impairments in dual diagnoses of gambling and SUD.

Translational Psychiatry (2026)16:245; <https://doi.org/10.1038/s41398-026-04015-4>

INTRODUCTION

Decision-making impairments are a defining feature of various psychiatric disorders, including gambling disorder (GD) and substance use disorder (SUD) [1]. GD and SUD frequently co-occur, worsening cognitive and behavioral deficits, particularly those associated with impulsivity and risk-taking behavior [2, 3]. For instance, individuals with GD often show higher rates of nicotine dependence and alcohol use disorder, along with greater gambling severity, compared to the general population [4–6]. Additionally, cocaine and amphetamine use are associated with GD, reinforcing the connection between substance use and gambling [7, 8]. To investigate the neurobiological basis of these decision-making impairments, researchers utilize standardized behavioral paradigms. The Iowa Gambling Task (IGT) is a widely used neuropsychological tool for assessing such deficits in humans by evaluating choices under uncertainty, reward, and punishment [9, 10]. Translating these concepts into animal research, a rat gambling task (rGT) which utilizes sucrose pellets (reward) and timeouts (punishment) with varying probabilities was developed, allowing researchers to investigate the underlying neural mechanisms [11–14].

Neuroimaging studies of the human brain have demonstrated that frontostriatal pathways, particularly those connecting the prefrontal cortex (PFC) and nucleus accumbens (NAc), are crucial in regulating decision-making [15, 16]. Impaired decision-making, in turn, is associated with disruptions such as diminished frontostriatal activity and altered prefrontal dopamine levels [15–17], with cocaine abusers showing persistent functional abnormalities in these crucial neural networks [16–19]. In rodent studies, chronic cocaine exposure is known to reliably alter decision-making processes. This is characterized by a dose-dependent increase in impulsive choice in delay-discounting tasks, leading to a preference shift toward immediate small rewards over delayed larger ones [20, 21]. A similar shift toward risky decision-making has also been observed in the rGT in previous studies, including our own [22–24]. Notably, Ferland and Winstanley (2017) demonstrated that the interaction between cocaine exposure and decision-making in the rGT may be influenced by factors such as baseline risk preference, the timing of assessment, and the presence of reward-paired cues, which can enhance both risk-preferring behavior and behavioral responses to cocaine [23].

¹Department of Physiology, Yonsei University College of Medicine, Seoul 03722, Republic of Korea. ²Department of Medical Sciences, Yonsei University College of Medicine, Seoul 03722, Republic of Korea. ³Present address: Nash Family Department of Neuroscience, Icahn School of Medicine at Mount Sinai, New York, NY 10029, USA.

✉email: maru0222@yuhs.ac; jkim1@yuhs.ac

Received: 22 June 2025 Revised: 23 February 2026 Accepted: 24 March 2026

Published online: 03 April 2026

These behavioral shifts result from profound neuroadaptations within the PFC-NAc circuitry [25, 26]. Among these neuroadaptations, chronic cocaine induces long-lasting changes in dopaminergic signaling [27], which plays a central regulatory role in risky decision-making. Chemogenetic inhibition of VTA dopamine neurons reduces risk preference in the rGT [28], while dopamine D1 and D2 receptors in the medial PFC exert distinct modulatory effects. D1 receptor overexpression induces maladaptive risk-taking [29], whereas D2 receptor modulation primarily facilitates flexible adjustments in choice behavior [30]. As a key target of neural projections from the mPFC, the NAc integrates cortical and limbic information to guide goal-directed behavior in a dopamine-dependent manner [31]. In particular, the prelimbic (PrL) subregion of the mPFC is vital for maintaining an optimal choice strategy, as its temporary inactivation impairs decision-making in the rGT [30], and the NAc core region contributes to the motivational aspects of decision-making [32, 33]. This PrL-NAc core pathway mediates cocaine-seeking behaviors, with c-Fos expression in this circuit correlating with cocaine seeking [34], and both optogenetic and chemogenetic inhibition of this pathway block this behavior [35, 36]. However, whether manipulating this pathway can reverse cocaine-induced risky decision-making remains unexplored.

To address this gap, we employed the rGT to assess decision-making while using designer receptors exclusively activated by designer drugs (DREADD) to selectively modulate PrL-NAc core pathway activity [37] with the potent agonist JHU37160 (J60) [38]. We examined the molecular mechanisms underlying these effects by analyzing DARPP-32, a key signaling hub where the D1 receptor pathway (activated by cocaine) and Gi-coupled pathway (activated by inhibitory DREADD) converge [37, 39, 40]. Our analysis focused on DARPP-32 phosphorylation at T34 and S97, along with PKA, GSK3 β (a D2-pathway marker) [41, 42], and the L-type calcium channel CaV1.2, which is implicated in cocaine-induced plasticity [43–45].

MATERIALS AND METHODS

Experimental design

This study was conducted in a sequential manner to investigate the role of the prelimbic cortex (PrL) to nucleus accumbens (NAc) core pathway in cocaine-induced risky decision-making. First, we performed a functional validation experiment using c-Fos immunohistochemistry to confirm that our chemogenetic (DREADD) manipulation could effectively modulate cocaine-induced neuronal activity in the target pathway under a behaviorally relevant timeline (Fig. 1). Following this validation, we conducted the main behavioral experiments (Fig. 2), where rats were trained on the rat gambling task (rGT) before undergoing either cocaine or no-cocaine exposure protocols combined with DREADD manipulations to assess changes in choice behavior (Fig. 2D). Finally, to explore the underlying molecular mechanisms, a subset of rats from the behavioral experiments underwent molecular analysis via Western blotting to examine protein expression changes in the PrL (Fig. 5A). Animals were randomly allocated to each experimental condition (e.g., DREADD virus type and cocaine/no-cocaine).

Animals

Male Sprague-Dawley rats (6 weeks old) were obtained from Orient Bio Inc. (Seongnam-si, Korea). They were housed two per cage in a 12 h light/dark cycle room (lights out at 8:00 pm), and all experiments were conducted during the daytime. To increase their motivation for the task, rats received a restricted diet that lowered their body weight to 85% of normal levels, which started 2 days before the pre-training experiments and was maintained until the end of the experimentation.

Drugs

Cocaine hydrochloride (Belgopia, Louvain-La-Neuve, Belgium) and JHU37160 (Hellobio, Bristol, UK) were dissolved in sterile 0.9% saline to a final concentration of 15 and 0.5 mg/kg, respectively.

Virus

Adeno-associated viruses (AAVs) (0.5 μ l; viral titer 7×10^{12} vg/ml) encoding either Cre-dependent hM4Di (pAAV-hSyn-DIO-hM4D(Gi)-mCherry) (Addgene, Watertown, MA, USA; the Addgene plasmid #44362 used to prepare this virus was a gift from Dr. Bryan Roth) or Cre-dependent hM3Dq (pAAV-hSyn-DIO-hM3D(Gq)-mCherry) (Addgene, Watertown, MA, USA; the Addgene plasmid #44361 used to prepare this virus was a gift from Dr. Bryan Roth) were infused bilaterally into the PrL for 5 min. Additionally, AAV (0.5 μ l; 7×10^{12} vg/ml) encoding retrograde Cre recombinase (pENN-AAV-hSyn-Cre-WPRE-hGH) (Addgene, Watertown, MA, USA; the Addgene plasmid #105553 used to prepare this virus was a gift from Dr. James M. Wilson) was infused bilaterally into the NAc core. The complete experimental schemes are illustrated in Fig. 1A.

Stereotaxic surgery for virus infusion

Rats were anesthetized with intraperitoneal (IP) ketamine (100 mg/kg) and xylazine (6 mg/kg) and placed in a stereotaxic instrument with the incisor bar at 5.0 mm above the interaural line. After making an incision on the skin, the skull surface was exposed and infusion cannulas (28 gauge, Plastics One, Roanoke, VA, USA) connected to 1 μ l Hamilton syringes (Reno, NV, USA) via PE-20 tubing were angled at 10° to the vertical line and aimed at the PrL (A/P, +3.2; L, +1.3; D/V, -4.0 mm from bregma and skull) and the NAc core (A/P, +3.2; L, +2.8; D/V, -7.1 mm from bregma and skull). Virus infusions were conducted by an infusion pump at a rate of 0.1 μ l/min. The infusion cannulas were slowly removed after an additional 5 min to allow for viral diffusion. After viral injection, rats were returned to their home cages for a 2-week recovery period.

Animal treatment and tissue collection for c-Fos analysis

Rats received viral injections of Cre-dependent Gi or Gq-DREADD on the PrL and retrograde Cre recombinase on the NAc core. After 6 weeks, rats were administered with saline or cocaine (15 mg/kg, IP) followed by saline or J60 (0.5 mg/kg) injection with 45 min interval. After another 45 min, the rats were deeply anesthetized with ketamine (100 mg/kg) and xylazine (6 mg/kg) and then perfused transcardially with 10 mM PBS (pH 7.4) followed by 4% paraformaldehyde solution. Further details regarding tissue processing and immunostaining are described in the Supplementary Information.

c-Fos cell-counting analysis and histology

About 10 images co-labeled with c-Fos and NeuN were acquired each from the PrL and the NAc core. The images that had inappropriate signals or damaged regions were excluded from the final data. All images were acquired under the LSM710 confocal laser scanning microscope (Carl Zeiss, Oberkochen, Germany) with a 405 nm laser diode for NeuN, and a 488 nm argon laser for c-Fos. The thickness of the images was 6 μ m and obtained using a 20x objective (numerical aperture 0.8) with 0.6x digital zoom. All images were taken with a resolution of 1024 pixels in x-y dimensions. Cell-counting was performed using Zen desk software (Carl Zeiss), which semi-automatically counted the number of NeuN cells and a portion of them including c-Fos expression. Minimum areas of the cells containing c-Fos or NeuN signals were optimized according to the size of the cells or signals in the PrL and NAc core and fixed during all analyses. A threshold of each image was manually set up depending on the quality of the image. The level of NeuN or c-Fos expression was manually assessed. All analysis was conducted by an experimenter blind to the experimental groups.

Behavioral procedures

Pre-training. The detailed procedure for rGT training was described in our previous work [46] and data collection was automated using touchscreen operant chambers (Campden Instruments Ltd., Leics, UK). Detailed description about apparatus can be found in Supplementary Information. Briefly, animals were trained once daily in 30 min sessions, five days per week. Sucrose pellets (45 mg) (Bio-Serv, Flemington, NJ, USA) were used as rewards. During the pre-training period (stages 1–4), rats learned to associate touching a lit window with reward delivery and to recognize punishment (time-out) for inaccurate, omitted, or premature (impulsive) responses. Rats that achieved >80% accuracy and <20% omissions were considered to have acquired the task successfully, and they underwent DREADD virus insertion surgery (see Fig. 2A).

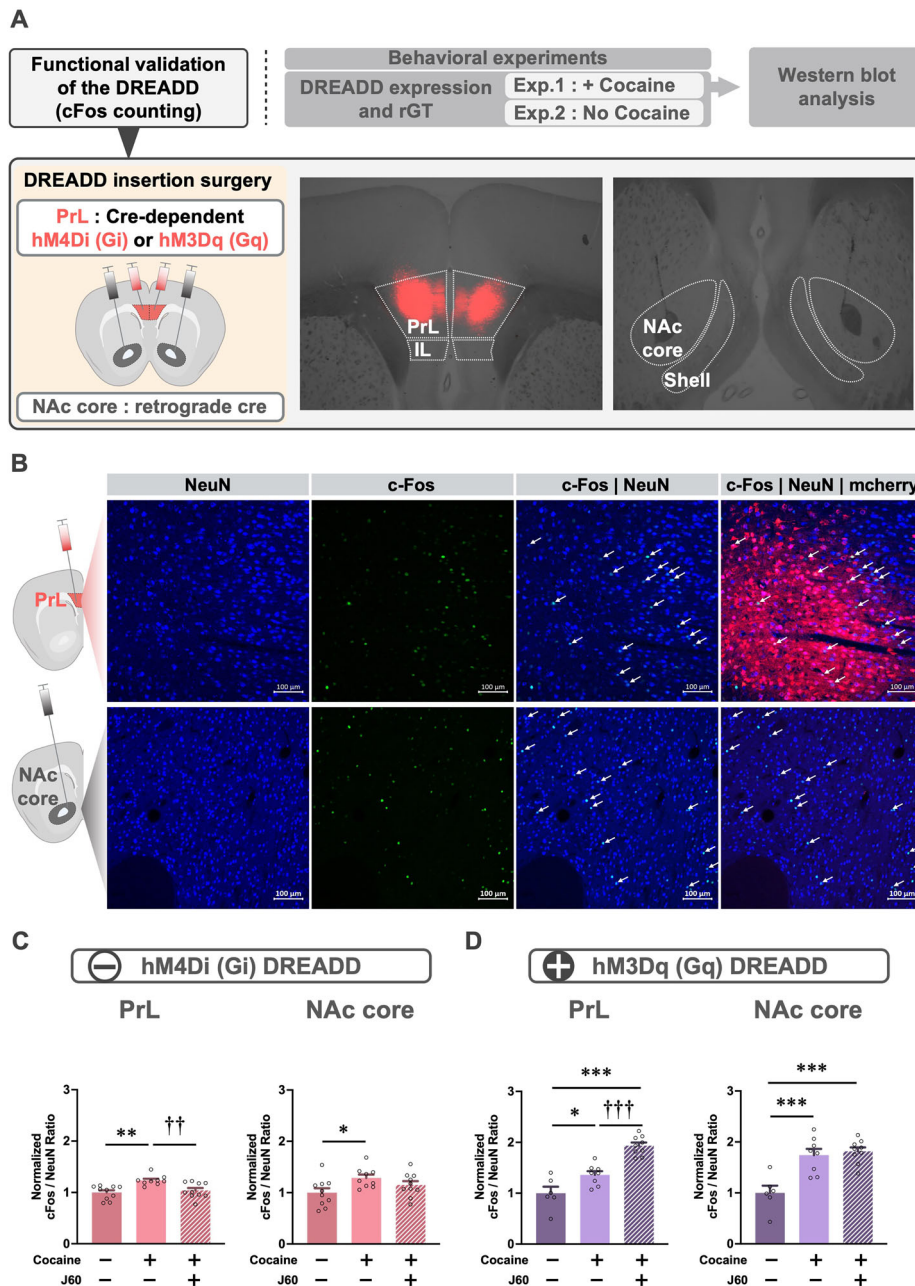


Fig. 1 Functional validation of DREADD-mediated modulation of neuronal activity in the PrL-NAc core pathway using c-Fos expression.

A The schematic illustration of the overall experimental workflow, beginning with the functional validation of DREADD activity (c-Fos counting) shown in this figure, which preceded the main behavioral experiments. To selectively express DREADDs in the PrL-NAc core pathway, Cre-dependent mCherry-tagged DREADDs (hM4Di-Gi or hM3Dq-Gq) were injected into the prelimbic cortex (PrL), while a retrograde Cre virus was injected into the nucleus accumbens (NAc) core. The representative image shows mCherry-tagged DREADD expression (red fluorescence) localized within the PrL, confirming expression in projection-specific neurons. **B** Representative confocal images from the PrL and NAc core show NeuN-positive neurons (blue) and c-Fos expression (green). The merged [c-Fos | NeuN] image demonstrates that c-Fos was quantified only within neurons (white arrows). The [c-Fos | NeuN | mcherry] merge displays DREADD-expressing neurons in relation to the other markers. Images were captured at 20x magnification. Scale bar = 100 μ m. **C** The graphs in C and D represent the ratio of c-Fos to NeuN, normalized to the Saline-saline control group. In Gi-DREADD expressing rats, cocaine administration significantly increased c-Fos levels in the PrL (** $P < 0.01$). Subsequent activation with J60 significantly attenuated this cocaine-induced increase ($\dagger\dagger P < 0.01$). In the NAc core, cocaine also induced a significant increase in c-Fos (* $P < 0.05$), which remained unaffected by J60. **D** Consistent with the excitatory function of Gq-DREADD, cocaine-induced elevation of c-Fos in the PrL (* $P < 0.05$) was further enhanced by J60 administration ($\dagger\dagger\dagger P < 0.001$). In the NAc core, cocaine induced a significant increase in c-Fos (** $P < 0.01$), which remained unaffected by J60. Data are presented as mean \pm SEM. The numbers of rats are as follows: Gi-sal-sal (n = 10), Gi-coc-sal (n = 9), Gi-coc-J60 (n = 10), Gq-sal-sal (n = 6), Gq-coc-sal (n = 8), Gq-coc-J60 (n = 9). Created with Biorender.com.

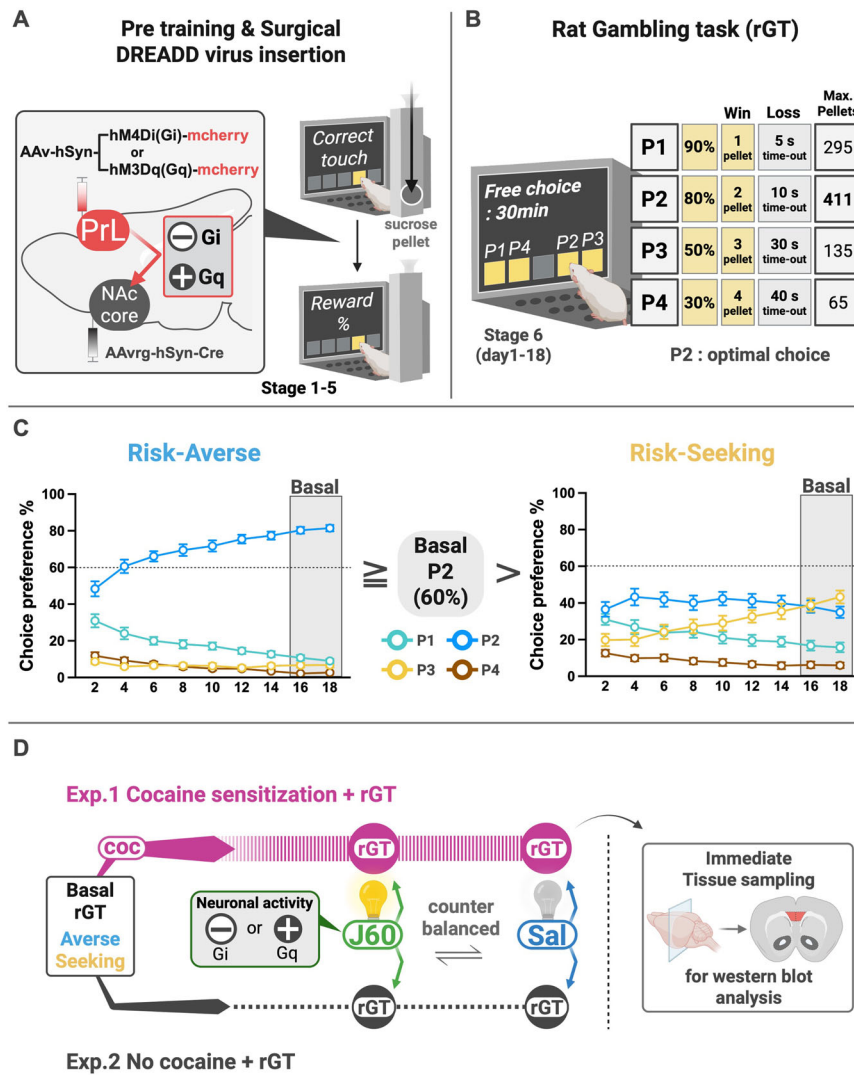


Fig. 2 Schematic illustration of the behavioral experiment procedures and groupings by choice preference after rGT. **A** Schematic illustration of the pre-training and surgery. Following pre-training to perform a correct touch for sucrose pellet rewards, rats underwent viral insertion surgery for projection-specific DREADD expression in the PrL-NAc core pathway. **B** Illustration of the rGT. During 30 min free-choice, rats freely select among P1–P4 options, each associated with different amounts of reward (1–4 sucrose pellets) and punishments (timeout durations). P2 is considered as an optimal choice because it yields the maximum number of pellets when only P2 choice was selected during the rGT. **C** Displayed are representative combined data of the choice preference scores obtained during the 18 consecutive days (even days only; mean ± S.E.M.) of rGT (stage 6) from Experiment 1 (Gi-DREADD only). Rats were categorized as risk-averse (left) when their basal score for P2 was equal to or higher than 60%, whereas they were categorized as risk-seeking (right) when their basal score for P2 was lower than 60%. The number of rats was 32 for the risk-averse group and 31 for the risk-seeking group. **D** Schematic illustration depicts the whole behavioral experiment. After the categorization of rats as risk-averse or risk-seeking was completed, the rats underwent cocaine sensitization + rGT (Experiment 1), or No cocaine + rGT (Experiment 2). In Experiment 1, the effect of cocaine and subsequent modulation of PrL-NAc core activity on rGT performance was evaluated in a counterbalanced manner. In Experiment 2, the effect of PrL-NAc core activity modulation during rGT was assessed without prior cocaine treatment. Immediately after the final rGT session, the rats were sacrificed, and brain tissue from a subset of them was collected for western blot analysis. Created with Biorender.com.

rGT

After two-weeks of recovery period, the rats were introduced to stage 5, where they learned that each of the four windows was associated with distinct reward and punishment probabilities: window P1 (1 pellet with 90% or 5 s time-out with 10%); window P2 (2 pellets with 80% or 10 s time-out with 20%); window P3 (3 pellets with 50% or 30 s time-out with 50%); and window P4 (4 pellets with 30% or 40 s time-out with 70%). In Stage 6, all four windows were simultaneously lit, allowing the rats to make free choices among them. The reward and punishment settings for each window in this stage were consistent with those introduced in stage 5, along with the ITI and stimulus duration time. Depending on the window they chose, rats received reward (pellets) or punishment (time-out) with differently programmed probabilities. Stage 6 continued until 18 daily sessions. To avoid any location bias, windows were allocated in a

counterbalanced way as follows: for half of the animals, the windows were 1 (P1), 2 (P4), 3 (P2), and 4 (P3); for the other half of the animals, the windows were 1 (P4), 2 (P1), 3 (P3), and 4 (P2).

Categorization of groups according to the choice preference

Hypothetically, if one window is chosen exclusively, the amount of reward pellets per session that an animal can obtain is as follows: P1, 295; P2, 411; P3, 135; and P4, 65 pellets. Among these options, P2 was considered the most optimal for maximizing overall rewards. After 18 daily sessions were completed, the average of the last three daily sessions' P2 choice percentages ([the number of P2 choices divided by the total number of choices] x 100) was considered a basal score for the risk preference. Rats were categorized as risk-averse when their basal score for P2 was equal to

or higher than 60%, whereas they were categorized as risk-seeking when their basal score for P2 was lower than 60%.

Design and procedures of behavioral experiments

Experiment 1 (effects of neuronal activity modulation on choice preference in the rGT with cocaine sensitization): After rGT stage 6, rats underwent a 7-day cocaine pre-exposure phase (15 mg/kg, IP, daily). This regimen was chosen for its proven efficacy in inducing neuroplasticity and behavioral sensitization [22, 47], which we further validated via plasticity-related molecules (e.g., CaV1.2 and DARPP-32) in the PrL (see Results). On Days 1 and 7, they received a cocaine injection in a cage outside the colony room, followed by the rGT session 60 min later. The 60-min interval was chosen to minimize high omission rates and task failure associated with the peak psychomotor effects of cocaine, ensuring reliable task performance while preserving the drug's effect on decision making [22]. On Days 2–6, they only received cocaine injections in their home cages. Upon completing cocaine pre-exposure, five to seven days of reminder rGT sessions were performed during the 2 weeks of withdrawal phase. This withdrawal period allows for the development of cocaine-induced metaplasticity, whereby synaptic adaptations remain functionally latent during abstinence but are primed for behavioral expression upon subsequent challenge [26]. After the withdrawal period, a challenge rGT session was conducted. During this session, cocaine was administered first, followed by the DREADD agonist J60 (0.5 mg/kg, IP) or saline administration 45 min later; the rGT session was conducted 15 min after the second injection (totaling 60 min post-cocaine). After seven days, J60 or saline injection following cocaine challenge was switched in a counterbalanced manner, and rGT was performed again (see Fig. 3A for the whole scheme).

Experiment 2 (effects of neuronal activity modulation on choice preference in the rGT with no cocaine): After completing stage six of the rGT, the J60 pre-exposure period began. This period followed a cocaine sensitization schedule, where the rats received a daily injection of J60 (0.5 mg/kg, IP) for seven consecutive days. On Days 1 and 7, the rats received a J60 injection 15 min before the rGT session, whereas on the remaining days, they only received J60 injections in their home cages. Once the J60 pre-exposure period was completed, five to seven days of reminder rGT sessions were conducted during the 2 weeks of the withdrawal phase. After the withdrawal period ended, challenge rGT was administered. During this session, the rats received saline first; a J60 or saline injection 45 min later; an rGT session was conducted 15 min later. Three days later, a counterbalanced challenge session was held in the same manner (see Fig. 3C for the whole scheme).

Western blot analysis

Some Gi-DREADD expressed rats used in Experiment 1 were decapitated right after the last counterbalanced rGT was completed. Additional rats separately trained and completed stage 6 of rGT were also decapitated. Brains were rapidly removed, and coronal sections were obtained with an ice-cold brain slicer (1 mm thick extending 1.60–2.60 mm from bregma). The Dual Fluorescent Protein (DFP) flashlight from NIGHTSEA (1560 Industry Rd, Hatfield, PA 19440, USA) was used for histological analysis detecting mCherry red fluorescent expressed rats in PrL region, after which the fluorescent-positive tissues were obtained bilaterally. Further details are provided in the Supplementary Information.

Statistical analysis

Data were shown as mean + standard error of the mean (SEM), and they were analyzed using GraphPad Prism (version 10.3) and R. Sample sizes were based on previous studies [22, 46]. While no a priori power analysis was performed, effect size calculations confirmed the adequacy of the sample size to detect the medium-to-large effects (Cohen's $f > 0.25$ – 0.28) observed in our main experimental groups. Unpaired t-test was used to compare the mean basal level expression of risk-averse and risk-seeking rats in western blot analysis. One-way analysis of variance (ANOVA) was used to compare the c-Fos+ neurons in cell counting or molecular expressions following cocaine and J60 administration in western blot. One-way repeated ANOVA measure was used to analyze the preference change within a single group across experimental phases (e.g., Basal, Pre-exposure, Challenge). Two-way repeated ANOVA measure was used to compare the preference scores following cocaine and subsequent DREADD agonist (J60) injection. This analysis was also applied to the delta-from-basal. ANOVAs were followed by *post hoc* Tukey or Bonferroni multiple comparison test.

Differences between experimental conditions were considered statistically significant when $p < 0.05$.

RESULTS

All statistical details analyzed for the results are summarized in Supplemental Tables.

Validation of projection-specific chemogenetic modulation in the PrL-NAc core pathway

To selectively manipulate the PrL-NAc core pathway, we employed a dual-viral approach combining Cre-dependent DREADD expression in the PrL with retrograde Cre delivery from the NAc core (Fig. 1A). This strategy enabled projection-specific expression of either inhibitory (hM4Di-Gi) or excitatory (hM3Dq-Gq) DREADDs in PrL neurons projecting to the NAc core. Confocal imaging confirmed mCherry-tagged DREADD expression within the PrL and validated that c-Fos quantification was restricted to NeuN-positive neurons in both the PrL and NAc core (Fig. 1B).

To validate functional efficacy, we examined whether DREADD activation could bidirectionally modulate cocaine-induced c-Fos expression. In Gi-DREADD expressing rats, cocaine significantly increased c-Fos in the PrL ($P < 0.01$), which was successfully suppressed to baseline levels by J60 administration ($P < 0.01$) (Fig. 1C). Conversely, in Gq-DREADD expressing rats, J60 further enhanced cocaine-induced c-Fos elevation in the PrL ($P < 0.01$) (Fig. 1D). This bidirectional modulation was specific to the PrL, as the NAc core remained unaffected by J60. This finding suggests that chemogenetic modulation of only the PrL input may be insufficient to reduce the overall elevation of c-Fos expression by cocaine in NAc core neurons. Nonetheless, these results indicate that our chemogenetic strategy provides effective regulation over cocaine-induced neuronal activity in the PrL region.

Categorization of groups according to the choice preference in rGT

As illustrated in Fig. 2A, the rats underwent pre-training, followed by surgical insertion of the viruses and subsequently underwent rGT training until their preference choices stabilized (Fig. 2B). Over 18 consecutive days of measurement, rats were categorized as risk-averse ($P2 \geq 60\%$) or risk-seeking ($P2 < 60\%$) based on their choice preference for the optimal P2 option during the last three days of the task (Fig. 2C). Risk-averse rats consistently preferred the advantageous P2 option from the beginning, whereas risk-seeking rats showed fluctuating preferences initially but increasingly favored the disadvantageous P3 option as the task progressed. The rats were then divided into two experimental groups. In Experiment 1, rats underwent cocaine sensitization and neuronal activity modulation of the PrL-NAc core pathway, followed by performance assessment on the rGT. In Experiment 2, rats underwent only pathway activity modulation prior to the rGT, without cocaine exposure.

Attenuation of cocaine-induced increase in risk-choice preference by Gi-DREADD, but not Gq-DREADD, activation in pre-categorized risk-averse rats

To investigate whether PrL-NAc core pathway modulation regulates cocaine-induced risky decision-making, we compared choice preferences following cocaine challenge to baseline scores (Experiment 1; Fig. 3A and S1A). In risk-averse rats expressing either Gi- or Gq-DREADDs (Fig. 3B), cocaine significantly reduced optimal choice preference (P2; $P < 0.01$ – 0.001) and increased risky choices (P3 and P4; $P < 0.05$ – 0.001). However, Gi-DREADD activation with J60, but not Gq-DREADD activation, significantly attenuated these cocaine-induced shifts for the P2 and P3 options ($P < 0.01$), demonstrating that inhibiting the PrL-NAc core pathway activity effectively reverses

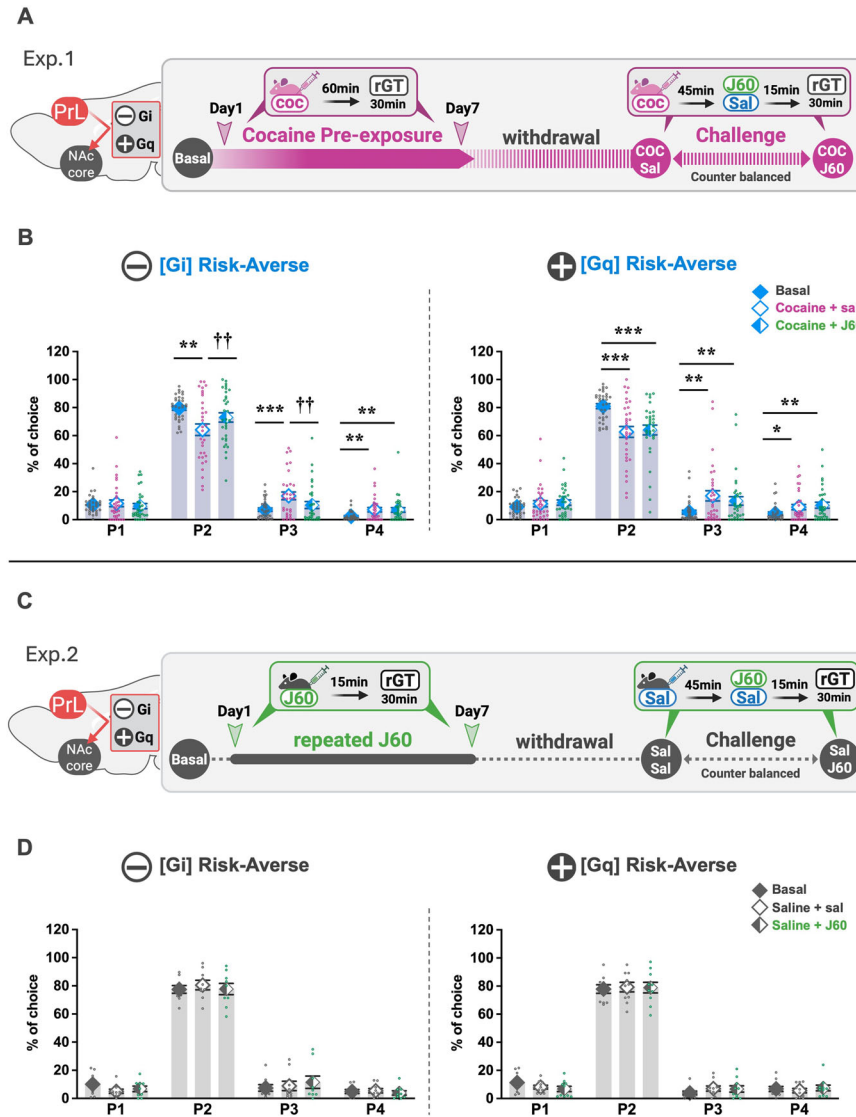


Fig. 3 Activation of Gi, but not Gq, DREADD in the PrL attenuates cocaine-induced increase of choice preference toward risk-seeking in basal risk-averse rats. **A** Schematic illustration depicts the procedure of experiment 1. Rats expressing Gi or Gq DREADDs in the PrL-NAc core pathway underwent a cocaine sensitization protocol starting right after the completion of rGT stage 6. Choice preference tests were performed during the cocaine pre-exposures (Day1 and 7), followed by 5–7 consecutive normal rGT during withdrawal period. During the challenges, rGT was performed after cocaine with saline or cocaine with J60 administration in a counter-balanced manner. **B** The percentages of choice preference on two cocaine challenge days (with or without J60) were compared to basal choice preference score calculated as the average of the last three days of choice preference scores in stage 6. In risk-averse rats, cocaine significantly reduced P2 choices and increased P3 and P4 choices compared to basal score. However, these effects were attenuated by J60 administration in rats with Gi-DREADD but not in rats with Gq-DREADD $***P < 0.001$, $**P < 0.01$, $*P < 0.05$, $\dagger P < 0.01$, compared to cocaine only. Data are shown as mean + SEM. The numbers of rats are as follows: Gi-Averse ($n = 32$) and Gq-Averse ($n = 33$). **C** Schematic illustration depicts the procedure of experiment 2. Rats expressing Gi or Gq DREADDs in the PrL-NAc core pathway were repeatedly injected with J60 alone similar to the cocaine sensitization protocol starting right after the completion of rGT stage 6. Choice preference tests were performed during the J60 pre-exposures (Day1 and 7), followed by 5–7 consecutive normal rGT. During the challenges, rGT was performed following saline or J60 administration in a counter-balanced manner. **D** The percentages of choice preference on two challenge days were compared to basal choice preference score that was calculated as the average of the last three days of choice preference scores in stage 6. J60 produced no significant changes in choice preference compared to basal score. Data are shown as mean + SEM. The numbers of rats are as follows: Gi-Averse ($n = 9$) and Gq-Averse ($n = 10$). Created with Biorender.com.

cocaine-induced risk-seeking. In contrast, risk-seeking rats showed no cocaine-induced alterations in choice preference, and neither Gi- nor Gq-DREADD activation modified their decision-making (Fig. S1B).

Beyond choice preference, cocaine increased omission rates and reward collection latency compared to baseline in both phenotypes (Figs. S3 and S4). DREADD activation generally did not reverse these effects, although Gi-DREADD partially mitigated cocaine-induced omission increases.

To determine whether chronic modulation of this pathway alone affects decision-making, we next examined rats receiving repeated J60 administration in the absence of cocaine (Experiment 2; Fig. 3C and S1C). Under no-cocaine conditions, repeated J60 treatment alone did not produce any significant change in choice preference compared with basal levels in either group (Fig. 3D and S1D). However, activation of Gq-DREADDs slightly reduced premature responses (Fig. S4B), suggesting a distinct role of excitatory PrL-NAc core activity.

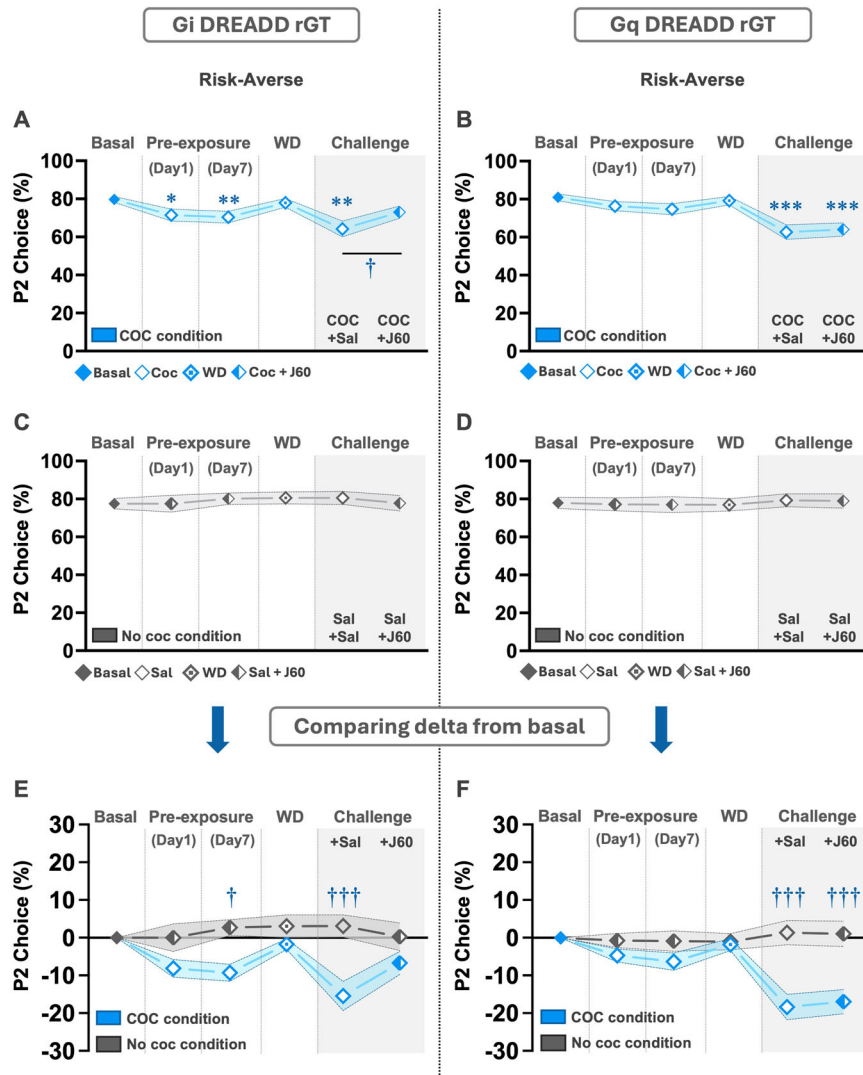


Fig. 4 Longitudinal effects of cocaine on P2 choice and its differential modulation by Gi- and Gq-DREADD activation in risk-averse rats. Changes in P2 choice percentage are presented across all experimental phases through the longitudinal analysis, comparing the Cocaine condition (blue lines) with the No-cocaine condition (grey lines). **A** In Gi-DREADD expressing rats, P2 choice% was significantly reduced from Basal during cocaine pre-exposure (Day 1, * $P < 0.05$; Day 7, ** $P < 0.01$). This reduction was restored during the withdrawal period (WD) and re-emerged during the cocaine challenge with saline (** $P < 0.01$). Subsequent activation of Gi-DREADD with J60 significantly inhibited this cocaine-induced shift ($\dagger P < 0.05$ compared to the cocaine + saline challenge). **B** In Gq-DREADD expressing rats, P2 choice was significantly reduced from Basal during the cocaine challenge, an effect that was present with both saline and J60 administration (** $P < 0.001$). **C-D** In the No-cocaine condition, activation of either Gi- or Gq-DREADD alone did not produce significant changes in P2 choice. **E** In Gi-DREADD expressing rats, a delta-from-basal analysis revealed that the Cocaine condition showed a significantly lower P2 choice compared to the No-cocaine condition at Pre-exposure Day 7 ($\dagger P < 0.05$) and during the challenge without DREADD activation ($\dagger\dagger\dagger P < 0.001$). This difference between conditions was abolished following J60 administration. **F** In the Gq-DREADD groups, the delta-from-Basal analysis showed a sustained and significant reduction in P2 choice for the Cocaine condition compared to the No-cocaine condition at both challenges with saline and J60 ($\dagger\dagger\dagger P < 0.001$). Data are presented as mean \pm SEM. The numbers of rats are as follows: Cocaine condition [Gi-Averse ($n = 32$), Gq-Averse ($n = 33$); No-cocaine condition [Gi-Averse ($n = 9$), Gq-Averse ($n = 10$)].

Longitudinal effects of cocaine on P2 choice and its differential modulation by Gi and Gq-DREADD activation

To examine whether PrL-NAc core pathway activity regulates cocaine-induced changes in risk-taking behavior, we performed a longitudinal analysis of P2 choice across all experimental phases, comparing the cocaine (Experiment 1) and no-cocaine (Experiment 2) conditions (Fig. 4 and S2).

In risk-averse rats, the cocaine condition induced dynamic changes in choice behavior that were dependent on the type of DREADD modulation (Fig. 4). In Gi-DREADD expressing rats, cocaine pre-exposure significantly reduced the preference for the P2 choice on both Day 1 ($P < 0.05$) and Day 7 ($P < 0.01$). This reduction was restored during the drug-free withdrawal period

but re-emerged during the cocaine challenge with saline ($P < 0.01$). Critically, Gi-DREADD activation with J60 significantly attenuated this cocaine-induced shift ($P < 0.05$), suggesting that inhibiting the PrL-NAc core pathway can reverse cocaine's effects on risk preference. In contrast, Gq-DREADD expressing rats showed significant reductions in P2 choice only during the cocaine challenge, with both saline and J60 producing comparable effects ($P < 0.001$) (Fig. 4B), indicating that pathway excitation did not mitigate cocaine-induced behavioral changes.

In the no-cocaine condition, P2 choice remained stable throughout all phases, regardless of DREADD activation (Fig. 4C-D), similar to the performance of saline treatment alone (Fig. S9). Therefore, we conducted a delta-from-basal analysis to directly

compare the two conditions (Fig. 4E–F). In the Gi-DREADD group, the cocaine condition showed significantly lower P2 choice at pre-exposure Day 7 ($P < 0.05$) and during the challenge without DREADD activation ($P < 0.001$), differences that were abolished by J60 administration (Fig. 4E). In the Gq-DREADD group, the cocaine condition maintained significantly lower P2 choice during both challenges regardless of J60 administration ($P < 0.001$) (Fig. 4F).

In contrast, risk-seeking rats displayed an inflexible choice pattern that was largely unaffected by either cocaine or DREADD modulation (Fig. S2A–D), with delta-from-basal analysis revealing no significant differences between conditions at any timepoint (Fig. S2E–F). These findings demonstrate that inhibiting the PrL-NAc core pathway specifically reverses cocaine-induced shifts in risk preference in risk-averse individuals.

Cocaine-induced molecular alterations in risk-averse rats resembling risk-seeking profiles and reversal by Gi-DREADD activation in the PrL

To elucidate molecular mechanisms underlying cocaine-induced preference shifts, we performed western blot analysis on PrL tissue collected immediately after the final rGT session (Fig. 5A). The analysis focused on identifying basal differences between risk-averse and risk-seeking rats and evaluating the effects of cocaine treatment (with or without J60) within each group.

We first examined the levels of the voltage-dependent L-type calcium channel $\alpha 1C$ subunit (CaV1.2). Although basal levels did not differ between the two groups, cocaine exposure significantly increased CaV1.2 expression in risk-averse rats ($P < 0.05$) and this increase was attenuated by concurrent Gi-DREADD activation ($P < 0.05$) (Fig. 5B). These molecular changes were not observed in risk-seeking rats.

Next, we examined the ratio of phosphorylated to total dopamine- and cAMP-regulated phosphoprotein, 32 kDa (DARPP-32). Under basal conditions, risk-seeking rats exhibited significantly higher total DARPP-32 levels (Fig. 5C) and a lower ratio of phosphorylated DARPP-32 at serine 97 (pS97) to total DARPP-32 (Fig. 5D) compared to risk-averse rats ($P < 0.05$). Notably, cocaine significantly reduced this ratio in risk-averse rats, similar to the level observed in risk-seeking rats ($P < 0.01$), whereas this effect was significantly increased to basal levels by concomitant Gi-DREADD activation ($P < 0.05$) (Fig. 5D). These changes were not observed in risk-seeking rats. We also examined other molecules, including CaV1.3, and the ratio of phosphorylation at threonine (T) 34 to total DARPP-32; however, no significant changes were observed in either the risk-averse or risk-seeking rats (Fig. 5S). Representative Western blot images are shown in Fig. 56.

To examine if these molecular changes were associated with preference for optimal choice (P2), we conducted correlation analyses under different treatment (basal, cocaine alone, and cocaine with J60). As a result, no significant correlations were observed between CaV1.2 and P2 (Fig. 57). However, a significant positive correlation was found between pDARPP-32(S97)/DARPP-32 and the P2 choice ($r = 0.62$, $P = 0.04$) with cocaine alone, whereas this effect disappeared with concomitant J60 administration in risk-averse rats (Fig. 5E). No significant correlations were found in risk-seeking rats (Fig. 5F).

Consistent with the behavioral analysis shown in Fig. 3B, the rats used for the molecular experiments exhibited the cocaine-induced risky decision-making and its reversal by Gi-DREADD activation in risk-averse rats (Fig. 58).

DISCUSSION

Modulation of cocaine-induced risky decision-making by the PrL-NAc core pathway in risk-averse rats

Chronic cocaine use influences the activity of the PrL-NAc core pathway [34–36], and also drives decision-making toward risky

options [22]. In the present study, we demonstrated that the inhibition of neuronal activity by Gi-DREADD activation in the PrL-NAc core pathway can attenuate the cocaine-induced increase of preference for risky options in risk-averse rats (Fig. 3B left). Notably, decision-making impairment was not evident during withdrawal, yet became pronounced following a cocaine challenge (Fig. 4A–B). This phenomenon can be explained by the concept of “cocaine-induced metaplasticity”, where drug-induced neuroadaptations remain latent during abstinence but rapidly re-emerge upon drug re-exposure [26], providing a critical window for our intervention with Gi-DREADD activation.

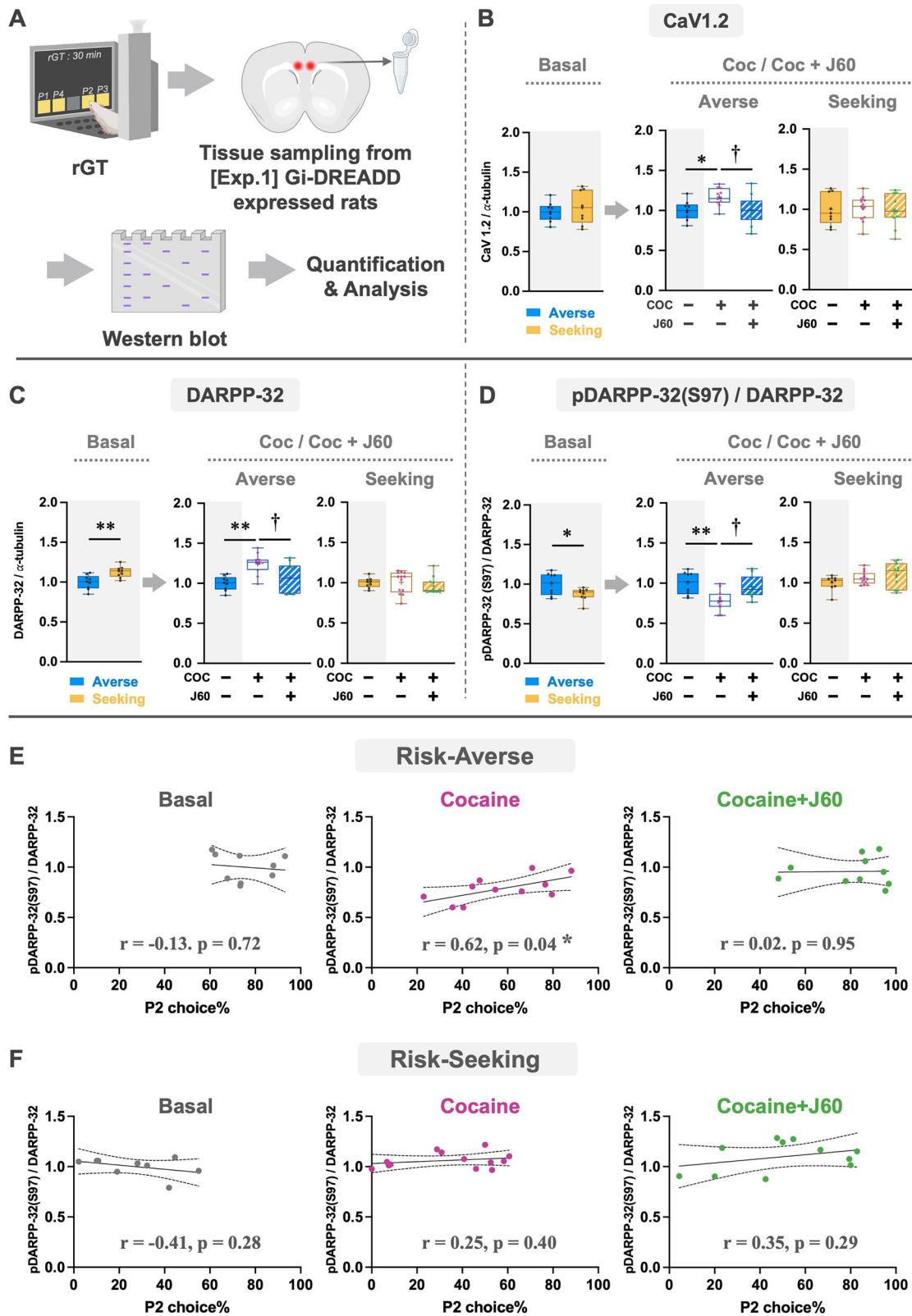
However, excitatory Gq-DREADD activation failed to alter the cocaine-induced risk preference in risk-averse rats, despite increasing PrL neuronal activity (Fig. 1D). Furthermore, risk-seeking rats displayed an inflexible response, as their decision-making was unaffected by either cocaine or subsequent DREADD activity modulation (Fig. S1B). Even in the absence of cocaine, repeated activation of both Gi- and Gq-DREADD in the PrL-NAc core pathway did not affect risky decision-making (Fig. 3D and S1D), demonstrating that pathway modulation specifically interacts with cocaine-induced neuroadaptations rather than affecting baseline risk preferences. Delta-from-basal analysis further confirmed that cocaine significantly reduced P2 choice compared to the no-cocaine condition, a difference abolished by Gi-DREADD but not Gq-DREADD activation (Fig. 4E–F).

Beyond risk preference, pathway-specific intervention affected other behavioral parameters. Gi-DREADD activation, but not Gq-DREADD, partially prevented cocaine-induced increases in omission rates in risk-averse rats (Fig. S3A), suggesting that the PrL-NAc core pathway mediates attentional processes in task engagement [48]. These results raise the possibility that the PrL-NAc core pathway mediates the influence of attention on decision-making in certain populations. In contrast, Gq-DREADD activation suggests a potential modulatory role on impulsive behavior as shown by decreased premature responses in the no-cocaine condition (Fig. S4B), rather than on decision-making (Fig. 3B, D), which aligns with recent evidence demonstrating that activation of the mPFC-NAc pathway reduces motor impulsivity [49].

DARPP-32 and CaV1.2 as molecular determinants of cocaine-induced risk preference in the PrL

Our molecular analysis in the PrL revealed two critical findings. First, baseline DARPP-32 signaling differed between risk-averse and risk-seeking rats, with the latter exhibiting constitutively higher total DARPP-32 levels and lower pDARPP-32(S97)/DARPP-32 ratios (Fig. 5C–D). Remarkably, cocaine exposure in risk-averse rats replicated this molecular profile, shifting their pDARPP-32(S97) ratio to levels resembling risk-seeking rats—a shift reversed by Gi-DREADD activation (Fig. 5D). The positive correlation between P2 choice and pDARPP-32(S97)/DARPP-32 ratio specifically in cocaine-treated risk-averse rats ($r = 0.62$, $P = 0.04$) (Fig. 5E), but not in risk-seeking rats (Fig. 5F), demonstrates that S97 phosphorylation serves as a molecular determinant of risky decision-making. While pDARPP-32(T34)/DARPP-32 ratios remained stable across groups (Fig. 5S5B), increased total DARPP-32 in cocaine-treated risk-averse rats (Fig. 5C) implies elevated T34 phosphorylation. Since D1 receptor activation increases T34 while decreasing S97 phosphorylation, resulting in DARPP-32 nuclear translocation [40, 41], cocaine-induced behavioral changes likely occur through D1 receptor signaling in the PrL. Unchanged GSK3 β levels (Fig. 5S5F), a D2 signaling marker, support the D1 pathway specificity.

In addition to DARPP-32 dysregulation, cocaine significantly increased CaV1.2 expression in risk-averse rats, an effect mitigated by Gi-DREADD activation (Fig. 5B, middle). CaV1.2, a key component of L-type calcium channels, modulates neuronal excitability through calcium influx and plays a pivotal role in cocaine sensitization [43–45]. This suggests that it may contribute



to cocaine-induced increases in preference for risky options in pre-categorized risk-averse rats by lowering the threshold for synaptic changes linked to risk-seeking behavior. In contrast, CaV1.3, another LTCC subtype, did not show any change in expression after cocaine exposure or Gi-DREADD activation (Fig. S5A),

suggesting that CaV1.2 plays a central role in the cocaine-induced risk-preference changes.

This mechanism also accounts for why Gq-DREADD failed to alter cocaine effects. Cocaine already drives the PrL-NAc core pathway toward excessive D1 receptor activation, and further excitatory

Fig. 5 Activation of Gi-DREADD in the PrL modulates cocaine-induced differential expression of CaV1.2 and DARPP-32 in risk-averse rats. **A** The illustration depicts whole experimental procedures. After completion of rGT with cocaine challenge (with or without J60), brain slices were made and the PrL regions were punched out, followed by protein analysis using Western blot. **B** In risk-averse rats, cocaine significantly increased CaV1.2 expression levels compared to basal group (* $P < 0.05$), whereas it was significantly reduced by subsequent administration of J60 ($\dagger P < 0.05$). No difference was observed in risk-seeking rats. **C** A significant increase in total DARPP-32 expression was observed in risk-seeking compared to risk-averse rats (** $P < 0.01$). Cocaine administration in risk-averse rats significantly increased total DARPP-32 levels (** $P < 0.01$), whereas J60 attenuated this effect ($\dagger P < 0.05$) in risk-averse rats. No difference was observed in risk-seeking rats. **D** A significant decrease in the ratio of phosphorylated DARPP-32 at S97 to total DARPP-32 was observed in risk-seeking compared to risk-averse rats (* $P < 0.05$). Cocaine administration in risk-averse rats also significantly decreased this ratio (** $P < 0.01$), whereas J60 attenuated this effect ($\dagger P < 0.05$) in risk-averse rats. No difference was observed in risk-seeking rats. **E** Scatter plots illustrate the correlation between P2 choice and the ratio of phosphorylated DARPP-32 at S97 to total DARPP-32 for each animal in risk-averse group, with Pearson's r and p -values. A positive correlation was observed in cocaine-treated rats ($r = 0.6209$, * $P < 0.05$), while this correlation was absent in basal and cocaine + J60 treated rats. **F** No significant correlation was observed between P2 choice and pDARPP-32(S97)/total DARPP-32 in risk-seeking rats. The numbers of rats for western blot analysis are as follows: Averse-Basal ($n = 9$), Averse-Coc ($n = 11$), Averse-Coc+J60 ($n = 10$), Seeking-Basal ($n = 9$), Seeking-Coc ($n = 13$), Seeking-Coc+J60 ($n = 11$). Created with Biorender.com.

modulation through Gq-DREADD cannot reverse or mitigate this overactivated state. Instead, inhibitory modulation via Gi-DREADD is required to normalize the hyperactive D1 signaling induced by cocaine. Notably, a subgroup of risk-seeking rats used for molecular analysis showed improved optimal choice with Gi-DREADD activation (Fig. S8), suggesting heterogeneity within the risk-seeking group. This finding indicates that some individuals classified as risk-seeking may retain sufficient molecular plasticity to benefit from pathway inhibition, warranting further investigation into the molecular determinants of this variability.

Implications for individualized treatment in SUD and GD

Our findings provide insights into individual differences in treatment responsiveness observed in human SUD and GD populations. Clinical studies consistently report substantial variability in long-term outcomes, with relapse rates of 40–60% within the first year following treatment [50]. This variability is paralleled by our observation that only risk-averse rats exhibited reversible shifts in decision-making following cocaine exposure, whereas risk-seeking rats showed no response to pathway modulation. These results suggest that baseline neural circuit properties may contribute to differences in therapeutic responsiveness, though validation in clinical populations will be essential.

Our dissociation between Gi-DREADD effects (rescuing risky decision-making) and Gq-DREADD effects (reducing premature responding) aligns with clinical evidence that impulsivity comprises distinct dimensions, including risky decision-making and motor impulsivity, that map onto different neural substrates [51, 52]. These findings suggest that prefrontal-striatal pathway modulation differentially affects specific impulsivity dimensions depending on the direction of modulation.

Several factors warrant consideration in translating these findings. The heterogeneity observed within the risk-seeking group (Fig. S8), combined with known effects of sex [53, 54] and environmental factors such as social isolation [22] on risk preference, indicates that additional variables likely modulate treatment responsiveness. This study was conducted exclusively in male rats, and future work should include both sexes given well-documented sex differences in risk-taking and cocaine responsiveness. Furthermore, while our data showed no detectable alterations in decision-making parameters during repeated J60 injection (Fig. 4 and S9), which aligns with the reported biological neutrality of J60 [38], we acknowledge as a significant limitation that the potential long-term biological adaptations following repeated J60 administration cannot be definitively excluded. Therefore, future studies should include concurrent vehicle and DREADD ligand control groups within the same cohort and employ more comprehensive control conditions to rigorously validate the inert nature of chemogenetic ligands across experimental contexts.

Nonetheless, this study provides proof-of-concept that baseline behavioral characteristics reflect underlying molecular profiles that

predict intervention efficacy, offering a framework for investigating neurobiologically-informed treatment approaches in addiction.

DATA AVAILABILITY

The raw data supporting the conclusion of this article will be made available by the authors, without undue reservation. Correspondence and requests for materials should be addressed to Wha Young Kim or Jeong-Hoon Kim.

CODE AVAILABILITY

The code used for analysis is available from the corresponding author on reasonable request.

REFERENCES

- Orsini CA, Moorman DE, Young JW, Setlow B, Floresco SB. Neural mechanisms regulating different forms of risk-related decision-making: Insights from animal models. *Neurosci Biobehav Rev.* 2015;58:147–67.
- Chen S, Yang P, Chen T, Su H, Jiang H, Zhao M. Risky decision-making in individuals with substance use disorder: A meta-analysis and meta-regression review. *Psychopharmacology.* 2020;237:1893–908.
- Potenza MN, Balodis IM, Derevensky J, Grant JE, Petry NM, Verdejo-Garcia A, et al. Gambling disorder. *Nat Rev Dis Primers.* 2019;5:51.
- Kim SW, Grant JE, Eckert ED, Faris PL, Hartman BK. Pathological gambling and mood disorders: clinical associations and treatment implications. *J Affect Disord.* 2006;92:109–16.
- Dani JA, Harris RA. Nicotine addiction and comorbidity with alcohol abuse and mental illness. *Nat Neurosci.* 2005;8:1465–70.
- Hasin DS, Stinson FS, Ogburn E, Grant BF. Prevalence, correlates, disability, and comorbidity of DSM-IV alcohol abuse and dependence in the united states: results from the national epidemiologic survey on alcohol and related conditions. *Arch Gen Psychiatry.* 2007;64:830–42.
- Volkow ND, Koob GF, McLellan AT. Neurobiologic advances from the brain disease model of addiction. *N Engl J Med.* 2016;374:363–71.
- Ethier AR, Kim HS, Hodgins DC, McGrath DS. High rollers: correlates of problematic cocaine use among a community sample of gamblers. *J Gamb Stud.* 2020;36:513–25.
- Bechara A, Damasio AR, Damasio H, Anderson SW. Insensitivity to future consequences following damage to human prefrontal cortex. *Cognition.* 1994;50:7–15.
- Bechara A. Risky business: emotion, decision-making, and addiction. *J Gamb Stud.* 2003;19:23–51.
- Rivalan M, Ahmed SH, Dellu-Hagedorn F. Risk-prone individuals prefer the wrong options on a rat version of the iowa gambling task. *Biol Psychiatry.* 2009;66:743–9.
- Zeeb FD, Robbins TW, Winstanley CA. Serotonergic and dopaminergic modulation of gambling behavior as assessed using a novel rat gambling task. *Neuropsychopharmacology.* 2009;34:2329–43.
- van den Bos R, Koot S, de Visser L. A rodent version of the Iowa Gambling Task: 7 years of progress. *Front Psychol.* 2014;5:203.
- Kwak MJ, Choi SJ, Cai WT, Cho BR, Han J, Park JW, et al. Manipulation of radixin phosphorylation in the nucleus accumbens core modulates risky choice behavior. *Prog Neurobiol.* 2024;242:102681.
- Peters J, Vega T, Weinstein D, Mitchell J, Kayser A. Dopamine and risky decision-making in gambling disorder. *eNeuro.* 2020;7:ENEURO.0461–19.2020.

16. Grant JE, Odlaug BL, Chamberlain SR, Hampshire A, Schreiber LR, Kim SW. A proof of concept study of tolcapone for pathological gambling: relationships with COMT genotype and brain activation. *Eur Neuropsychopharmacol*. 2013;23:1587–96.
17. Balodis IM, Kober H, Worhunsky PD, Stevens MC, Pearson GD, Potenza MN. Diminished frontostriatal activity during processing of monetary rewards and losses in pathological gambling. *Biol Psychiatry*. 2012;71:749–57.
18. Bolla KI, Eldreth DA, London ED, Kiehl KA, Mouratidis M, Contoreggi C, et al. Orbitofrontal cortex dysfunction in abstinent cocaine abusers performing a decision-making task. *Neuroimage*. 2003;19:1085–94.
19. Verdejo-García A, Bechara A. A somatic marker theory of addiction. *Neuropharmacology*. 2009;56:48–62.
20. Dandy KL, Gatch MB. The effects of chronic cocaine exposure on impulsivity in rats. *Behav Pharmacol*. 2009;20:400–5.
21. Simon NW, Mendez IA, Setlow B. Cocaine exposure causes long-term increases in impulsive choice. *Behav Neurosci*. 2007;121:543–9.
22. Kim WY, Cho BR, Kwak MJ, Kim JH. Interaction between trait and housing condition produces differential decision-making toward risk choice in a rat gambling task. *Sci Rep*. 2017;7:5718.
23. Ferland JN, Winstanley CA. Risk-preferring rats make worse decisions and show increased incubation of craving after cocaine self-administration. *Addict Biol*. 2017;22:991–1001.
24. Cocker PJ, Rotge JY, Daniel ML, Belin-Rauscent A, Belin D. Impaired decision making following escalation of cocaine self-administration predicts vulnerability to relapse in rats. *Addict Biol*. 2020;25:e12738.
25. Dong Y, Nasif FJ, Tsui JJ, Ju WY, Cooper DC, Hu XT, et al. Cocaine-induced plasticity of intrinsic membrane properties in prefrontal cortex pyramidal neurons: adaptations in potassium currents. *J Neurosci*. 2005;25:936–40.
26. Lee BR, Dong Y. Cocaine-induced metaplasticity in the nucleus accumbens: silent synapse and beyond. *Neuropharmacology*. 2011;61:1060–9.
27. Wang X, Liu L, Adams W, Li S, Zhang Q, Li B, et al. Cocaine exposure alters dopaminergic modulation of prefronto-accumbens transmission. *Physiol Behav*. 2015;145:112–7.
28. Hynes TJ, Hrelja KM, Hathaway BA, Hounjet CD, Chernoff CS, Ebsary SA, et al. Dopamine neurons gate the intersection of cocaine use, decision making, and impulsivity. *Addict Biol*. 2021;26:e13022.
29. Beyer DKE, Horn L, Klinker N, Freund N. Risky decision-making following prefrontal D1 receptor manipulation. *Transl Neurosci*. 2021;12:432–43.
30. Zeeb FD, Baarendse PJ, Vanderschuren LJ, Winstanley CA. Inactivation of the prelimbic or infralimbic cortex impairs decision-making in the rat gambling task. *Psychopharmacology*. 2015;232:4481–91.
31. Goto Y, Grace AA. Limbic and cortical information processing in the nucleus accumbens. *Trends Neurosci*. 2008;31:552–8.
32. Stopper CM, Floresco SB. Contributions of the nucleus accumbens and its subregions to different aspects of risk-based decision making. *Cogn Affect Behav Neurosci*. 2011;11:97–112.
33. Ghods-Sharifi S, Floresco SB. Differential effects on effort discounting induced by inactivations of the nucleus accumbens core or shell. *Behav Neurosci*. 2010;124:179–91.
34. McGlinchey EM, James MH, Mahler SV, Pantazis C, Aston-Jones G. Prelimbic to accumbens core pathway is recruited in a dopamine-dependent manner to drive cued reinstatement of cocaine seeking. *J Neurosci*. 2016;36:8700–11.
35. Stefanik MT, Kupchik YM, Kalivas PW. Optogenetic inhibition of cortical afferents in the nucleus accumbens simultaneously prevents cue-induced transient synaptic potentiation and cocaine-seeking behavior. *Brain Struct Funct*. 2016;221:1681–9.
36. Siemsen BM, Barry SM, Vollmer KM, Green LM, Brock AG, Westphal AM, et al. A subset of nucleus accumbens neurons receiving dense and functional prelimbic cortical input are required for cocaine seeking. *Front Cell Neurosci*. 2022;16:844243.
37. Roth BL. DREADDs for Neuroscientists. *Neuron*. 2016;89:683–94.
38. Bonaventura J, Eldridge MAG, Hu F, Gomez JL, Sanchez-Soto M, Abramyan AM, et al. High-potency ligands for DREADD imaging and activation in rodents and monkeys. *Nat Commun*. 2019;10:4627.
39. Jenni NL, Larkin JD, Floresco SB. Prefrontal dopamine D(1) and D(2) receptors regulate dissociable aspects of decision making via distinct ventral striatal and amygdalar circuits. *J Neurosci*. 2017;37:6200–13.
40. Stipanovich A, Valjent E, Matamales M, Nishi A, Ahn JH, Maroteaux M, et al. A phosphatase cascade by which rewarding stimuli control nucleosomal response. *Nature*. 2008;453:879–84.
41. Nishi A, Matamales M, Musante V, Valjent E, Kuroiwa M, Kitahara Y, et al. Glutamate Counteracts Dopamine/PKA Signaling via Dephosphorylation of DARPP-32 Ser-97 and Alteration of Its Cytonuclear Distribution. *J Biol Chem*. 2017;292:1462–76.
42. Beaulieu JM, Gainetdinov RR, Caron MG. The Akt-GSK-3 signaling cascade in the actions of dopamine. *Trends Pharmacol Sci*. 2007;28:166–72.
43. Nasif FJ, Hu XT, White FJ. Repeated cocaine administration increases voltage-sensitive calcium currents in response to membrane depolarization in medial prefrontal cortex pyramidal neurons. *J Neurosci*. 2005;25:3674–9.
44. Ford KA, Wolf ME, Hu XT. Plasticity of L-type Ca²⁺ channels after cocaine withdrawal. *Synapse*. 2009;63:690–7.
45. Rajadhyaksha AM, Kosofsky BE. Psychostimulants, L-type calcium channels, kinases, and phosphatases. *Neuroscientist*. 2005;11:494–502.
46. Kwak MJ, Kim WY, Jung SH, Chung YJ, Kim JH. Differential transcriptome profile underlying risky choice in a rat gambling task. *J Behav Addict*. 2022;11:845–57.
47. Ku MJ, Kim CY, Park JW, Lee S, Jeong EY, Jeong JW, et al. Wireless optogenetic stimulation on the prelimbic to the nucleus accumbens core circuit attenuates cocaine-induced behavioral sensitization. *Neurobiol Dis*. 2024;203:106733.
48. Dalley JW, Laane K, Pena Y, Theobald DE, Everitt BJ, Robbins TW. Attentional and motivational deficits in rats withdrawn from intravenous self-administration of cocaine or heroin. *Psychopharmacology*. 2005;182:579–87.
49. Arrondeau C, Uruena-Mendez G, Marchessaux F, Goutaudier R, Ginovart N. Activation of the mPFC-NAC pathway reduces motor impulsivity but does not affect risk-related decision-making in innately high-impulsive male rats. *J Neurosci Res*. 2024;102:e25387.
50. McLellan AT, Lewis DC, O'Brien CP, Kleber HD. Drug dependence, a chronic medical illness: implications for treatment, insurance, and outcomes evaluation. *JAMA*. 2000;284:1689–95.
51. MacKillop J, Weafer J, Gray JC, Oshri A, Palmer A, de Wit H. The latent structure of impulsivity: impulsive choice, impulsive action, and impulsive personality traits. *Psychopharmacology*. 2016;233:3361–70.
52. Verdejo-García A, Lawrence AJ, Clark L. Impulsivity as a vulnerability marker for substance-use disorders: review of findings from high-risk research, problem gamblers and genetic association studies. *Neurosci Biobehav Rev*. 2008;32:777–810.
53. van den Bos R, Jolles J, van der Knaap L, Baars A, de Visser L. Male and female Wistar rats differ in decision-making performance in a rodent version of the Iowa Gambling Task. *Behav Brain Res*. 2012;234:375–9.
54. Becker JB, McClellan ML, Reed BG. Sex differences, gender and addiction. *J Neurosci Res*. 2017;95:136–47.

ACKNOWLEDGEMENTS

This work was supported by the National Research Foundation of Korea funded by the Ministry of Science and ICT (2022R1A4A5033852, RS-2025-00563430, RS-2025-24873007).

AUTHOR CONTRIBUTIONS

Joonyeup Han: Writing – original draft, Validation, Methodology, Investigation, Formal analysis, Data curation, Conceptualization. Myung Ji Kwak: Methodology, Investigation, Formal analysis, Data curation, Conceptualization. Wha Young Kim: Writing – original draft, Validation, Supervision, Methodology, Investigation, Funding acquisition, Formal analysis, Data curation, Conceptualization. Jeong-Hoon Kim: Writing – original draft, Validation, Supervision, Methodology, Investigation, Funding acquisition, Formal analysis, Data curation, Conceptualization.

COMPETING INTERESTS

The authors declare no competing interests.

ETHICS APPROVAL AND CONSENT TO PARTICIPATE

All animal experiments and methods were performed in accordance with the relevant guidelines and regulations. The experimental protocols were approved by the Institutional Animal Care and Use Committee (IACUC) of Yonsei University College of Medicine (Approval No. A-2023-0176). As this study involved only animal subjects, requirements for informed consent from human participants and consent for publication of identifiable human images are not applicable.

ADDITIONAL INFORMATION

Supplementary information The online version contains supplementary material available at <https://doi.org/10.1038/s41398-026-04015-4>.

Correspondence and requests for materials should be addressed to Wha Young Kim or Jeong-Hoon Kim.

Reprints and permission information is available at <http://www.nature.com/reprints>

Publisher's note Springer Nature remains neutral with regard to jurisdictional claims in published maps and institutional affiliations.



Open Access This article is licensed under a Creative Commons Attribution-NonCommercial-NoDerivatives 4.0 International License, which permits any non-commercial use, sharing, distribution and reproduction in any medium or format, as long as you give appropriate credit to the original author(s) and the source, provide a link to the Creative Commons licence, and indicate if you modified the licensed material. You do not have permission under this licence to share adapted material derived from this article or parts of it. The images or other third party material in this article are included in the article's Creative Commons licence, unless indicated otherwise in a credit line to the material. If material is not included in the article's Creative Commons licence and your intended use is not permitted by statutory regulation or exceeds the permitted use, you will need to obtain permission directly from the copyright holder. To view a copy of this licence, visit <http://creativecommons.org/licenses/by-nc-nd/4.0/>.

© The Author(s) 2026